ECRONICON OPEN ACCESS

EC OPHTHALMOLOGY
Research Article

Quantification of Leukocyte Trafficking in a Mouse Model of Multiple Sclerosis through *In Vivo* Imaging

Fan Xia[1#], Jonathan L Lin[1,2#], David L Zhang[3#], Shuizhen Shi[1], Seth E Buscho[1] and Massoud Motamedi[1*]

[1]*Department of Ophthalmology and Visual Sciences, University of Texas Medical Branch, Galveston, Texas, USA*

[2]*Department of Pharmacology and Toxicology, University of Texas Medical Branch, Galveston, Texas, USA*

[3]*Clear Falls High School, League City, Texas, USA*

***Corresponding Author:** Massoud Motamedi, Department of Ophthalmology and Visual Sciences, University of Texas Medical Branch, Galveston, Texas, USA.

Received: September 09, 2022 ; **Published:** October 06, 2022

#These authors contributed equally to this work"

Abstract

Purpose: Optic neuritis occurring in multiple sclerosis (MS) is a disease characterized by chronic inflammation and demyelination in the optic nerve. Although it has been well appreciated that leukocyte infiltration into the optic nerve is an early event during the course of the disease, there has been no study on visualizing and quantifying leukocyte trafficking in the retina during the progression of MS.

Methods: In this study, we generated green fluorescent protein $(GFP)^+$ bone marrow chimeric mice, in which GFP-labeled leukocytes facilitate the visualization of their trafficking in the retina. This reporter was then integrated with a well-established rodent model for MS-experimental autoimmune encephalomyelitis (EAE), allowing high resolution *in vivo* scanning laser ophthalmoscopy (SLO) to track leukocyte movement in the retina in real time. Quantification of leukocyte trafficking was accomplished through Imaris software.

Results: Through SLO, we were able to localize the GFP signal, allowing us to clearly identify leukocytes within the vascular space. We observed more intense leukocyte migration in the retina of EAE mice, exhibiting three distinct movement behaviors: flowing, rolling/crawling and adherent. There was a marked increase in leukocyte rolling and adhesion in retinal vasculature, particularly in the veins and capillaries after induction of EAE. The velocity of rolling leukocytes ranged from 12.0 to 1065.0 μm/sec in the veins as compared to 14.1 to 942.0 in the capillaries. Furthermore, focal areas of recurrent leukocyte adhesion to endothelial surfaces were observed in EAE retinas.

Conclusion: We generated a novel model that makes it possible to non-invasively track leukocyte trafficking in the retina of EAE mice. Our study demonstrates that leukocyte migration in an MS model is distinctly different from the control, suggesting that leukocytes may play a key role in the development of retinal vascular inflammation and optic neuritis during MS, warranting further investigation of the pathological roles of leukocytes in the disease onset and progression.

Keywords: *Multiple Sclerosis (MS); Experimental Autoimmune Encephalomyelitis (EAE); In Vivo Imaging; Scanning Laser Ophthalmoscopy (SLO); Leukocyte Trafficking; Chimeric Mice*

Introduction

Multiple sclerosis (MS) is a chronic autoimmune disease in the central nervous system (CNS), characterized by inflammation, demyelination and neurodegeneration. It is the most common disabling neurological disease of young adults in particular women between 20 to 40 years of age, affecting nearly 450,000 individuals in the United States and more than 2 million people worldwide [1]. Clinical symptoms of MS include vision problems, movement disorders, dizziness, cognitive dysfunction, slurred speech and problems with sexual, bowel and bladder function [2]. In particular, optic neuritis is a major clinical feature that can lead to visual impairment or even blindness, affecting 30% - 70% of MS patients, and observed in up to 94% - 99% of patients examined at post-mortem through the presence of demyelinating plaques in the optic nerves [3].

Optic neuritis is an inflammation of the optic nerve [4]. It was previously thought that immune cells such as activated T cells attack the myelin sheath of the optic nerve, causing demyelination, dysfunction and degeneration of the optic nerve [4]. Optic nerve degeneration then retrogradely leads to the thinning of the nerve fiber layer, and degeneration and dysfunction of retinal ganglion cells (RGCs) [2,5], resulting in irreversible visual loss. However, a few recent studies suggest that demyelination-independent neurodegeneration also contributes to the pathology of optic neuritis during MS [6]. Currently, optic neuritis is treated by intravenous administration of steroid, which can effectively reduce inflammation and decrease recovery time during the acute phase, but has limited benefits for long-term RGC degeneration and visual protection [2,5,7]. However, in prior studies, the critical role of leukocyte migration has not been thoroughly evaluated. Therefore, it is necessary to further investigate the impact of these mechanisms on the onset and progression of RGC injury during optic neuritis.

In this study, we developed a mouse MS model-experimental autoimmune encephalomyelitis (EAE) with GFP-tagged leukocytes, enabling the application of continuous *in vivo* high-resolution imaging techniques for visualization and quantification of leukocyte trafficking in the retina. This provided the first evidence that aberrant leukocyte migration accompanies vascular inflammation in the retina in a mouse MS model, suggesting that leukocytes may mediate retinal neurodegeneration, independent of optic nerve degeneration.

Materials and Methods

Animals

C57BL/6J wild type (WT) mice (Stock No: 000664) and C57BL/6-EGFP (Stock No: 006567) were originally obtained from the Jackson Laboratory (Bar Harbor, ME) and subsequently bred in the animal care facility at the University of Texas Medical Branch [8]. All experimental procedures and use of animals were performed in accordance with the Association of Research for Vision and Ophthalmology Statement for the Use of Animals in Ophthalmic and Vision Research, and animal protocols were approved by the Institutional Animal Care and Use Committee at the University of Texas Medical Branch.

Bone marrow (BM) transplant

BM transplantation was performed as described previously [8,9]. Briefly, we irradiated WT mice, which served as recipients, at a dose of 8.5 Gy (850 rads) with a Gammacell 40 irradiator (MDS Nordion). The mouse head and eyes were protected with a lead shield during the procedure. BM cell suspensions were isolated from femurs and tibias of donor GFP mice. We then washed, counted, and resuspended cells in PBS. We then injected 200 µL of the cell suspension containing 1.0×10^7 cells into the recipient animal via tail vein within 24 hours after irradiation.

EAE model

After BM transplantation, WT mice (12 - 13 weeks) were subjected to EAE model using MOG35- 55/CFA EMULSION PTX kit (#EK2110, Hooke Laboratories, Lawrence, MA) following the instructions provided by the kit [2]. In brief, the emulsion was injected subcutaneously at two sites (left and right hind legs), 0.1 mL/site. Then, PTX was administered via intraperitoneal injection after 2 hours and 24 hours, respectively. Optic neuritis usually began at 2 weeks and peaked at 3 weeks after the induction of immunization [5].

Scanning laser ophthalmoscope (SLO)

Mice were deeply anesthetized by 100 mg/kg ketamine and 10 mg/kg xylazine (i.p.), and eyes were dilated by topical administration of tropicamide and phenylephrine. Then, mice were positioned on a platform with a heating pad to maintain body temperature. The Heidelberg Spectralis HRA system (Heidelberg Engineering, Franklin, MA) was used to image the mice *in vivo* and record the movement of GFP^+-tagged leukocytes at a frame rate of 5 frames/second using the settings for fluorescein angiography with a 55° field of view. Each steady image was compiled from 100 frames.

Image processing

Image processing were made using Imaris 9.9 software with the Fiji/ImageJ Plugin (Labkit) (Bitplane, Belfast, United Kingdom). Briefly, SLO images or video frames were imported into Imaris for quantitative analysis of leukocyte movement and adhesion through the built-in cell tracking features. When taking images with Spectralis, it averaged over 100 frames, therefore, only stationary fluorescent objects (i.e. adherent leukocytes) would be clearly visible, allowing for quantification of leukocyte adhesion. Adherent leukocyte density was calculated as the number of cells in either a retinal area (total retina or capillary bed) or along the length of a vessel, expressed as cells/mm^2 surface area or cells/mm vessel length, respectively, with the retinal areas and vessel lengths determined through built- in masking functions in Imaris. For measuring the speed of rolling leukocytes, Imaris software calculated an object leukocyte's track length (distance along the track from the first position to the last position of the cell), which was divided by the time elapsed to move that distance.

Statistics

Data were presented as mean ± standard error of the mean (SEM) and analyzed by student's t-test or two-way ANOVA. Statistical analysis was conducted using GraphPad Prism program (GraphPad Software Inc., La Jolla, CA). A p value < 0.05 was considered statistically significant.

Results

Leukocyte adhesion is increased in the retina of EAE mice

To examine the movement of leukocytes in the retina in EAE model, we generated BM chimeric mice which expressed GFP exclusively in blood leukocytes, making it possible to intimately visualize the real-time trafficking of leukocytes in retinal vessels through high resolution SLO imaging. To do so, WT mice were irradiated, but the head and eyes of these mice were covered with a lead shield for protection. This was successfully followed by transplanting BM cells from GFP transgenic mice into irradiated WT mice. At 4 weeks after BM transplantation, EAE model was induced in these mice. SLO retinal images were taken right before and 14 days after EAE, respectively (Figure 1A). As each image was a compilation of 100 frames, only stationary structures and cells in the retina, such as retinal vessels and firmly adherent leukocytes, were captured during image acquisition (Figure 1B). We observed that there were only a few leukocytes which sparsely attached to retinal vessels before EAE (pre-EAE), indicating there is no overt retinal inflammation in pre-EAE mice. In contrast,

at 14 days after EAE (post-EAE), GFP-labeled leukocytes exhibited dramatically increased adhesion to the endothelium, particularly in retinal veins and capillaries, indicating that the adhesion response was specific to the development of EAE.

To quantify the distribution of adherent leukocytes, the Imaris software was used to process and analyze SLO images (Figure 1C), in which each green dot indicates an adherent leukocyte. Total leukocytes captured by SLO (Figure 1C, upper panels), total surface area of retinal images, surface area of capillary bed (Red area in figure 1C, lower panels) and the length of veins were quantified, and the distribution of leukocytes was calculated. As shown in figure 1D-1F, the density of leukocytes in the total surface area was 0.92 ± 0.13 vs 11.96 ± 3.36 leukocytes/mm^2, the average number of leukocytes along retinal veins was 0.35 ± 0.16 vs 6.88 ± 1.16 leukocytes/mm, and the density of leukocytes distributed in capillary bed was 0.66 ± 0.26 vs 5.97 ± 1.85 leukocytes/mm^2 in pre-EAE and post-EAE retinas, respectively.

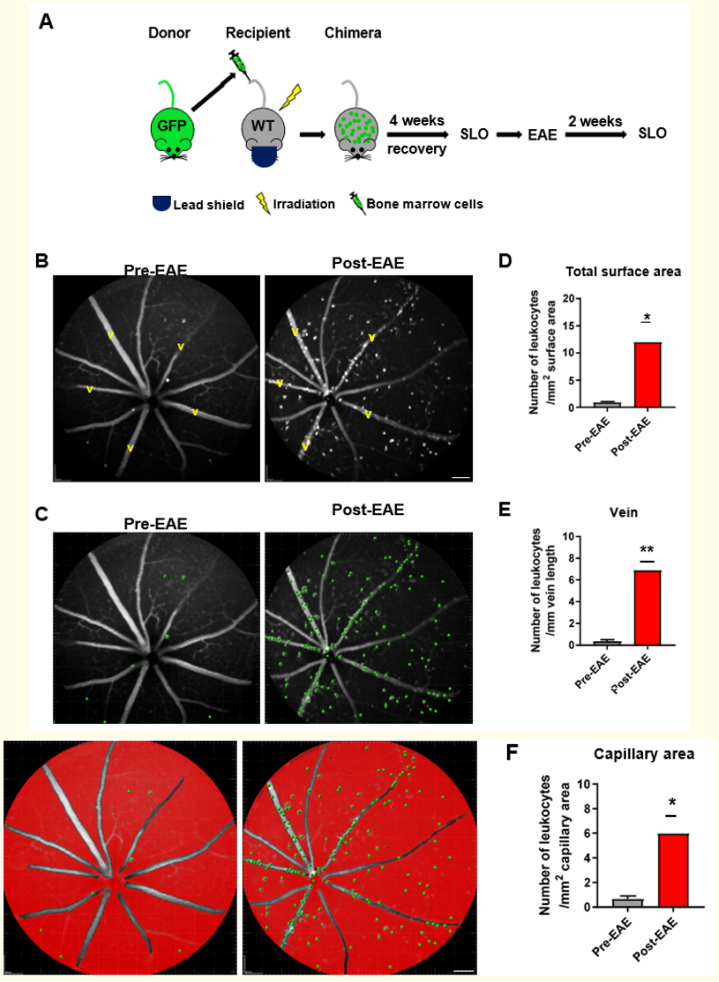

Figure 1: *Adherent leukocytes are increased in the retina of EAE model. (A) Schematic illustration for the generation of chimeric mice and experiment procedures. (B) Representative retinal images taken by SLO before and 14 days after EAE were shown. V: vein. (C-F) SLO images were processed and adherent leukocytes were quantified with Imaris software. Green dots indicate adherent leukocytes, and red color displays surface area. Scale bar: 200μm. n = 4; *p < 0.05 and **p < 0.01.*

Leukocyte behavior analysis in the retinas of EAE mice

To further assess the spatiotemporal dynamics of leukocyte movement in the retina of EAE mice, time- lapse movies were taken by SLO with an acquisition speed of 5 frames per second. Before EAE, the majority of leukocytes were moving quickly, accompanying the blood flowing through retinal blood vessels; therefore, leukocytes were barely detected and captured within the field of each SLO frame. In contrast, leukocytes were easily captured 14 days after the induction of EAE. To characterize the behaviors of leukocytes, five frames at fixed time intervals (1 second) were output from the SLO time- lapse movies (Figure 2A) and leukocytes in each frame were quantified by Imaris software (Figure 2B). Because each frame was a snapshot, counted leukocytes included stationary ones and those traveling at a relatively slower speed that allowed them to be captured in a frame (0.2 seconds). For leukocytes that were moving too fast, they resembled a line or a shooting star and were not counted. We found that the number of leukocytes captured in each SLO frame remained stable either in pre- EAE retinas or in the post-EAE retinas over a period of time (4 seconds), indicating relatively steady leukocyte kinetics. However, overall, compared with pre-EAE retinas, leukocytes captured in EAE retinas were markedly increased, indicating that EAE slowed leukocyte trafficking in the retina.

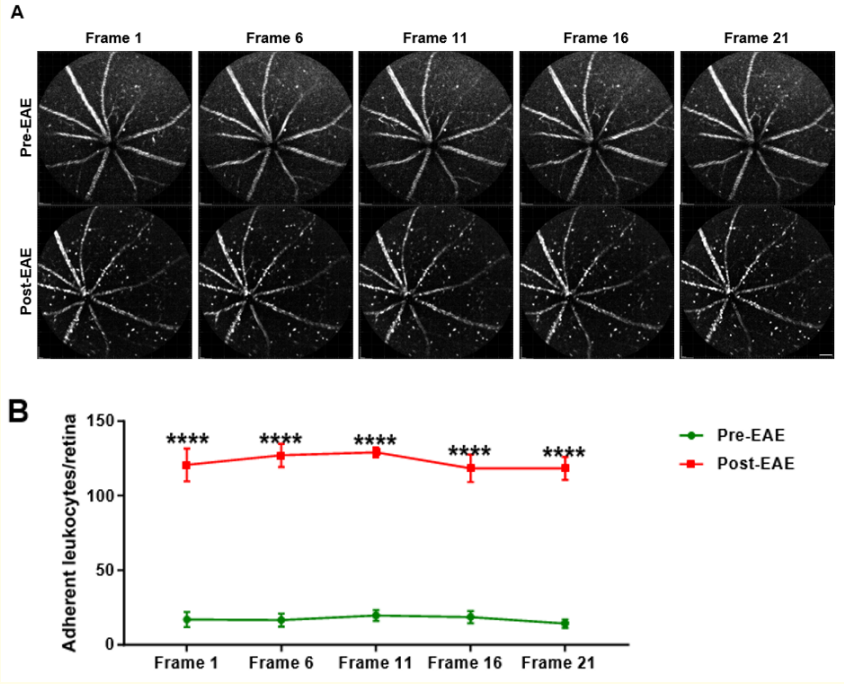

Figure 2: *The kinetics of leukocytes attachment in the retina of EAE model. (A) Representative retinal images taken by SLO before and 14 days after EAE at different time points. The display interval for images was 1 second and images were processed for background subtraction by Imaris software. (B) Adherent leukocytes were quantified with Imaris software. Scale bar: 200μm. n = 3; ****p < 0.0001.*

A closer examination of leukocyte actions during time-lapse acquisition of EAE retinas revealed that leukocytes displayed three distinct movement behaviors: flowing, rolling/crawling, and adherent (Figure 3A-3C). Leukocytes were classified as flowing if their velocity harmonized with the velocity of red blood cells (RBCs) through retinal vessels. Rolling/crawling leukocytes were identified if they

were adhering to the vessel walls and exhibited slower velocity than RBCs (Figure 3A-3B, yellow arrows). In addition, leukocytes were considered as firmly adherent if they were in stable contact with vascular endothelium and remained stationary during the observation time window (Figure 3A-3B, red arrowheads), while leukocytes were considered as loosely adherent if they had no movement for several seconds before starting to roll on the endothelium (Figure 3C). Furthermore, rolling/crawling leukocytes may be comprised of different subpopulations that have distinct migratory behavior and biological roles; therefore, we utilized Imaris software to calculate the velocity of rolling/crawling leukocytes in the capillaries and veins. The speed of rolling leukocytes ranged from 14.1 to 942.0 μm/sec in the capillary with the median speed of 145.8 μm/sec, and 12.0 to 1065.0 μm/sec in the vein with the median speed of 44.7 μm/sec, respectively (Figure 3D).

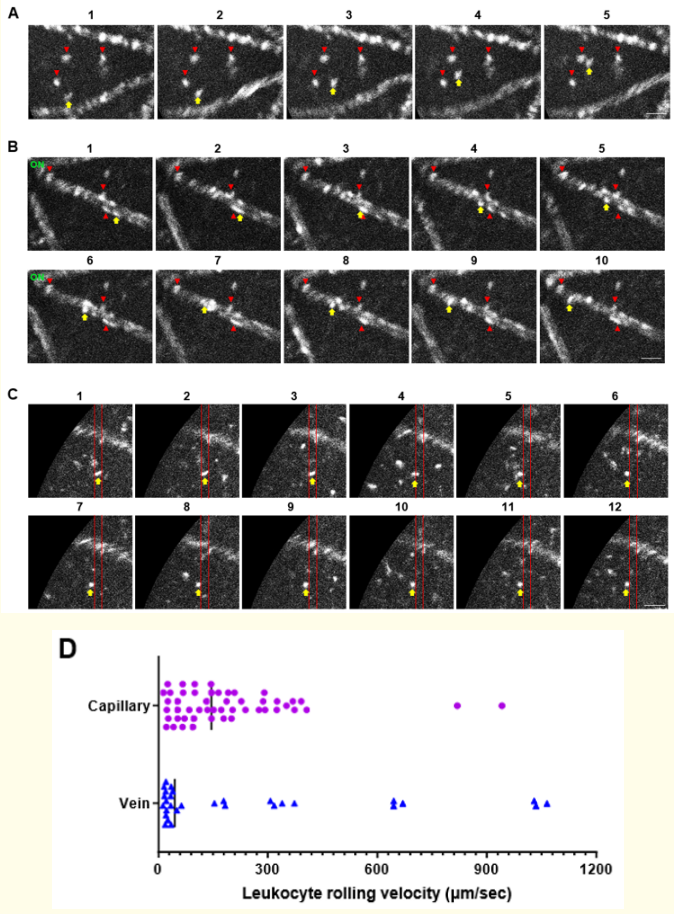

Figure 3: *The different behaviors of leukocytes in the retinal vasculature in EAE model. (A) Example of rolling and firmly adherent leukocytes in the capillary. Red arrowheads indicate attached leukocytes. Yellow arrow indicates rolling leukocyte. The display interval for images was 0.2 seconds. (B) Example of rolling and firmly adherent leukocytes in the vein. Red arrowheads indicate attached leukocytes. Yellow arrow indicates a rolling leukocyte. The display interval for images was 1 second. ON: optic nerve head. (C) Example of loosely adherent leukocytes in the capillary. Yellow arrow indicates a loosely adherent leukocyte. Red lines indicate the initial position of the loosely adherent leukocyte. The display interval for images was 2 seconds. (D) The speed of rolling leukocytes (30 leukocytes from vein and 50 leukocytes from capillary) was quantified by Imaris software. The black line indicates the median. Scale bar: 100μm.*

Interestingly, we also observed recurrent leukocyte rolling/crawling in some capillary beds (Figure 4A-4B, green circle), while no leukocytes were observed in other capillaries in the EAE retinas (Figure 4A-4B, purple oval) during the observation period. As shown in figure 4B, red arrowheads in the green circle annotated adherent leukocytes, and yellow arrow in the green circle noted a rolling leukocyte. In the first row of images (Frame 1-6), the leukocyte rolled in the capillary and finally flowed away with the circulation. After a while (Frame 27-32, 108-113), other leukocytes were captured rolling on the endothelium of the same area. As the literature suggests that when leukocytes crawl on the endothelium, they are actively searching suitable spots in preparation for adhesion and extravasation [10], we also observed the presence of "hotspots" where different leukocytes kept adhering to endothelium in EAE retinas. As shown in figure 4C-4D, several leukocytes lined up and slowly rolled on the endothelium (Frame 1-7), but they disappeared in Frame 8. However, other leukocytes later appeared and similarly rolled in this area (Frame 9-14). As leukocytes could block blood flow when they attached to capillaries, it is possible that the come-and-go action of leukocytes could induce repeated ischemia-reperfusion in these capillaries.

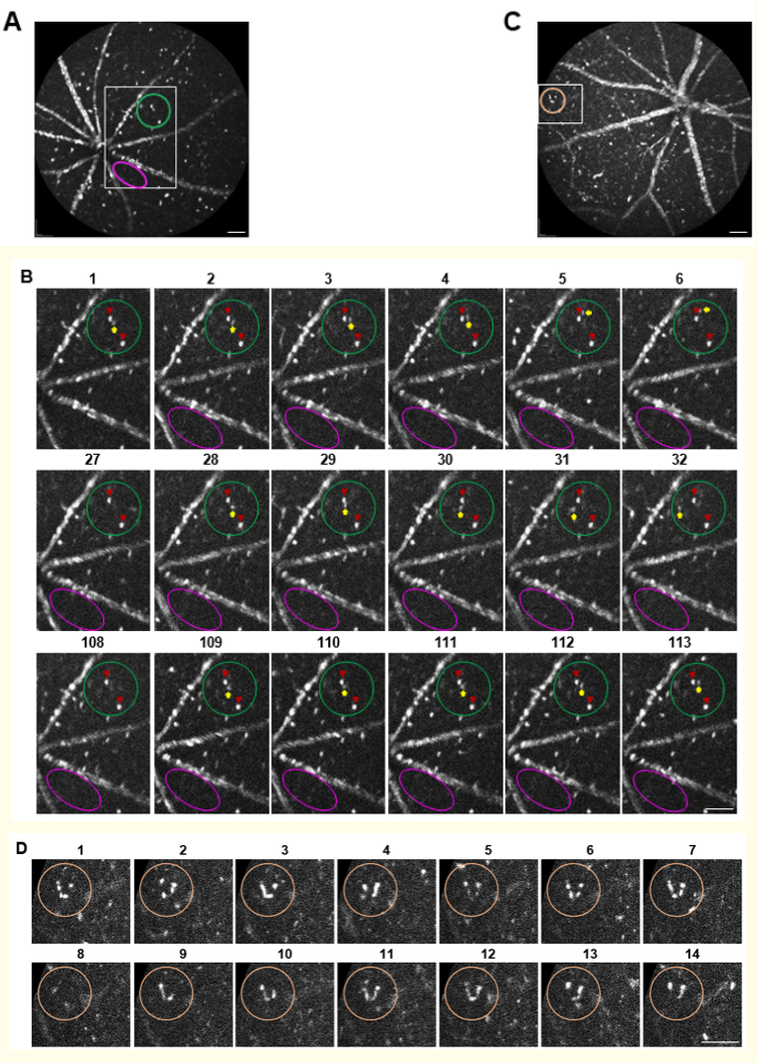

Figure 4: *Areas of recurrent leukocyte adhesion in the retinal vasculature in EAE model. (A-B) Example of recurrent leukocyte rolling/crawling area (green circle) and no leukocyte rolling/crawling area (purple oval) in EAE retina. White rectangle in (A) was zoomed in for leukocyte movement in (B), in which 3 rows of images were extracted from different time periods. The display interval for images was 0.2 seconds. Red arrowheads indicate attached leukocytes. Yellow arrow indicates a rolling leukocyte. (C-D) Example of hotspots of leukocyte rolling/crawling in the capillary of EAE retina (orange circle). White rectangle in (C) was zoomed in for leukocyte movement in (D). The display interval for images was 2 seconds. Scale bar: 200 µm.*

Discussion and Conclusion

Since optic neuritis occurring in MS is a chronic inflammatory and demyelinating disease in the optic nerve, it has been well appreciated that leukocyte infiltration into the optic nerve is an early event during the course of the disease [6,11-13]. Down-regulation of Treg cells and up-regulation of Th17 cells in the optic nerve are likely involved in RGC damage and optic nerve degeneration in this process [11]. However, there are currently no studies on the visualization and quantification of the actions of leukocytes trafficking in the retina during MS development. In this study, we generated GFP/WT chimeric mice and used high resolution *in vivo* SLO imaging to non-invasively observe leukocyte movement in the retina before and after inducing EAE. We provided the first evidence that leukocyte rolling and attachment to retinal vessels, which are typical features of vascular inflammation, were markedly increased in the EAE retinas. Moreover, in several capillaries, we observed temporary leukocyte attachment and detachment, which could block blood flow and then be followed by reperfusion. It is well-established that enhanced trafficking and adhesion of leukocytes could damage the neurovascular tissue by inducing repeated local ischemia-reperfusion releasing molecules such as proteases, matrix metalloproteinases, reactive oxygen species and proinflammatory cytokines [14] leading to inflammation and tissue damage, thus our findings suggest that increases in leukocyte rolling and attachment in retinal vessels may play a role in RGC injury in addition to retrograde RGC death induced by optic nerve degeneration. Additionally, the increase in the leukocyte migration and adhesion may impact the other inflammatory responses such as edema in the inner retinal layer and disruption of blood-retinal-barrier that are found at early onset of EAE [6].

At this moment, the underlying mechanisms of increased leukocyte rolling and attachment in the retinal vessels in EAE are not clear. Such phenomenon has been noted in diabetic retinopathy due to increased expression of vascular adhesion molecules such as ICAM-1 and their corresponding receptors on leukocytes such as CD18 [15,16]. Blocking the interaction between ICAM-1 and CD18 not only attenuates leukocyte attachment but also prevents the development of diabetic retinopathy [15,16]. Moreover, increased leukocyte rolling and attachment are found in RGC axonal injury induced by optic nerve crush (ONC) which is mediated by the upregulation of the CXCL10/CXCR3 pathway [8]. Nonetheless, in ONC model, leukocyte rolling and attachment occurs in veins near the optic nerve head while in our EAE model, such phenomenon was observed throughout veins as well as capillaries. Therefore, leukocyte rolling and attachment in EAE may not merely be the consequence of axonal injury. Future studies with single cell technology, histology and flow cytometry are needed to identify alterations in endothelial cells, leukocytes, neurons and glia, characterize subtypes of attached and rolling leukocytes and identify molecular mechanisms involved in this process.

To visualize leukocytes *in vivo*, we transplanted bone marrow from GFP mice to non-fluorescent WT mice to label leukocytes with green fluorescence while keeping retinal tissue non-fluorescent. Combined with high resolution SLO and image analysis through the Imaris software, this novel approach allowed us to successfully identify and quantify the motility of leukocytes in the EAE retinas at a relatively early stage of the disease. Our ongoing study is focused on analyzing leukocyte trafficking at different stages after the induction of EAE (3 - 60 days post EAE) and correlating the expected findings to the development and progression of retinal ischemia, vascular leakage, RGC dysfunction and death as well as optic nerve degeneration with the goal of further characterizing the critical role of leukocyte trafficking in the EAE pathology.

In summary, using novel real-time *in vivo* imaging of leukocyte trafficking in EAE model, we found a marked increase in leukocyte rolling and adhesion in retinal vessels in MS. Our study suggests that changes in leukocyte migration may play a key role in the induction of retinal vascular inflammation and optic neuritis during MS, warranting further investigation of the pathological roles of leukocytes in the disease and development of potential therapeutic intervention using emerging therapeutic agents.

Acknowledgments

This work was supported in part by Charles H. and Mary Campbell Professor in Ophthalmology and Visual Sciences Endowment Research Fund, and NIEHS T32 Training Grant Support T32ES007254.

Conflict of Interest Statement

There is no financial interest or conflict of interest.

Bibliography

1. Kaiser-Kupfer MI., *et al.* "Tamoxifen retinopathy". *Cancer Treatment Reviews* 62 (1978): 315e320.
2. Noureddin BN., *et al.* "Ocular toxicity in low-dose tamoxifen: a prospective study". *Eye* 13.6 (1999):729e733.
3. Gualino V., *et al.* "Optical coherence tomography findings in tamoxifen retinopathy". *American Journal of Ophthalmology* 140 (2005): 757e758.
4. Bourla DH., *et al.* "Peripheral retinopathy and maculopathy in high-dose tamoxifen therapy". *American Journal of Ophthalmology* 144 (2007):126-128.
5. Neuville J., *et al.* "Spectral domain OCT imaging techniques in tamoxifen retinopathy". *Optometry and Vision Science* 92 (2015): e55-59.
6. Baget-Bernaldiz M., *et al.* "Optical coherence tomography study in tamoxifen maculopathy". *Archivos de la Sociedad Española de Oftalmología* 83 (2008): 615-618.
7. Doshi RR., *et al.* "Pseudocystic foveal cavitation in tamoxifen retinopathy". *American Journal of Ophthalmology* 157 (2014): 1291e1298. e1293.
8. Rijal RK., *et al.* "Crystalline deposits in the macula-tamoxifen maculopathy or macular telangiectasia?" *Nepalese Journal of Ophthalmology* 6 (2014): 227e229.
9. Gass JD. "Histopathologic study of presumed parafoveal telangiectasis". *Retina* 20 (2000): 226-227.
10. Yannuzzi LA., *et al.* "Idiopathic macular telangiectasia". *Archives of Ophthalmology* 124 (2006): 450-460.
11. Koizumi H., *et al.* "Morphologic features of group 2A idiopathic juxtafoveolar retinal telangiectasis in three-dimensional optical coherence tomography". *American Journal of Ophthalmology* 142 (2006): 340-343.
12. Charbel Issa P., *et al.* "Confocal blue reflectance imaging in type 2 idiopathic macular telangiectasia". *Investigative Ophthalmology and Visual Science* 49 (2008): 1172-1177.
13. Maruko I., *et al.* "Early morphological changes and functional abnormalities in group 2A idiopathic juxtafoveolar retinal telangiectasis using spectral domain optical coherence tomography and microperimetry". *British Journal of Ophthalmology* 92 (2008): 1488-1491.
14. Powner MB., *et al.* "Perifoveal müller cell depletion in a case of macular telangiectasia type 2". *Ophthalmology* 117 (2010): 2407-2416.
15. Powner MB., *et al.* "Loss of Müller's cells and photoreceptors in macular telangiectasia type 2". *Ophthalmology* 120 (2013): 2344-2352.
16. Behrens A., *et al.* "Tamoxifen Use in a Patient with Idiopathic Macular Telangiectasia Type 2". *Case Reports Ophthalmology* 9.1 (2018): 54-60.
17. Lee S., *et al.* "OCT Angiography Findings of Tamoxifen Retinopathy: Similarity with Macular Telangiectasia Type 2". *Ophthalmology Retina* 3.8 (2019): 681-689.

18. Crisóstomo S., *et al.* "TAMOXIFEN-INDUCED CHORIORETINAL CHANGES: An Optical Coherence Tomography and Optical Coherence Tomography Angiography Study". *Retina* 40.6 (2020):1185-1190.

19. Yokoyama T., *et al.* "Unmeasurable small size of foveal avascular zone without visual impairment in optical coherence tomography angiography". *Eye* 32.6 (2018): 1062-1066.

20. Kanda Y. "Investigation of the freely available easy-to-use software 'EZR' for medical statistics". *Bone Marrow Transplant* 48.3 (2013): 452-458.

Volume 13 Issue 11 November 2022